Indian J Pure Appl Math (2026) 57:1747–1762
https://doi.org/10.1007/s13226-024-00687-0

ORIGINAL RESEARCH

Gold-blood nanofluid flow in cone-disk system for Tiwari and Das model in the presence of thermal radiation using lie group approach

Aarti Manglesh · **Rajeev Kumar** · **Tejinder Kumar**

Received: 18 November 2023 / Accepted: 20 August 2024 / Published online: 9 September 2024
© The Indian National Science Academy 2024, corrected publication 2026

Abstract The cone-disk system, featuring a cone in contact with a disk at its apex, is a versatile arrangement used in applications such as conical diffusers, viscosimeters and medical devices. Present research focus on the theoretical analysis of gold blood nanofluid flow in cone disk system for Tiwari and Das model in the presence of thermal radiation. The three dimensional axisymmetric gold blood nanofluid flow is analysed for four distinct models namely model I (rotating cone and static disk), model II (static cone and rotating disk), model III (co-rotating cone and disk) and model IV (counter rotating cone and disk). The governing non-linear equations are transformed to self similar equations by using one parameter Lie group approach and solved by using bvp5c package of MATLAB to examine the effect of different parameters involving in the problem. In order to validate the result, Nusselt number at cone and disk surfaces are compared with the published literature and the closed agreement authenticates the validation of the problem. The influence of various parameters on velocity and temperature profile of gold blood nanofluid has been discussed in detail for all four configurations of cone disk system for the gap angle $\frac{\pi}{4}$ and are shown graphically. The result of this analysis shows that there is a outward radial flow as a result of high centrifugal forces due to rotation of disk/cone. Also the velocity of nanofluid decrease with increasing the nanoparticle volume fraction. The results also reveal that an increase in the nanoparticle volume fraction, power exponent, and radiation parameter values leads to an increase in the temperature profile.

Keywords Nanofluid · Gold-Blood nanofluid · Tiwari and Das model · Lie-Group approach · Cone-disk system

1 Introduction

A Nanofluid is a special kind of fluid that consists of nano-sized particles dispersed within base fluid, such as water or oil. These naoparticles, which are extremely tiny, can improve the thermal and flow characteristics of the

Communicated by NM Bujurke.

Rajeev Kumar and Tejinder Kumar have contributed equally to this work.

A. Manglesh (✉)
International Centre for Distance Education and Open Learning, Himachal Pradesh University, Summer Hill, Shimla, Himachal Pradesh 171005, India
E-mail: dr.aartimanglesh@gmail.com

R. Kumar
Department of Evening Studies, The Mall, Himachal Pradesh University, Summer Hill, Shimla, Himachal Pradesh 171001, India
E-mail: rajeevkumar2012math@gmail.com

T. Kumar
Department of Mathematics and Statistics, Himachal Pradesh University, Summer Hill, Shimla, Himachal Pradesh 171005, India
E-mail: kumartejinder343@gmail.com

fluid. Nanofluids have lot of applications in microelectronics, biological and medical applications, administration of drugs and antibacterial therapies, fuel cell, solar systems, solar panels, thermal storage systems, cooling of electronic devices, etc [1]. The idea of nanofluids is adding solid particles of metals, carbides, and oxides into heat transfer fluids to enrich the thermal conductivity. This idea was given by Maxwell in 1873. When tiny solid particles (micrometer, millimeter) were mixed into the base fluids to enrich the thermal conductivity. They face some serious issues like clogging, increase in the pressure drop and the erosion of pipes. Nanofluids was first introduced by Choi and Eastman [2]. Choi [3] developed the nanofluid and demonstrated that a suspension of small particles with a volume fraction of less than 5% improves the heat production of fluids. Nanofluids are more stable than micro fluids and milli fluids. Base fluids behave more or less like pure fluids in the presence of nanoparticles thereby incurring very little pressure drop and eliminate the need for surfactants. They have distinctive properties like large surface area to volume ratio, properties that depend on dimension, lower kinetic energy and greater stability. The most curious property of nanofluid is that they show remarkable enhancement in thermal conductivity even by the addition of very small amounts of nanometer sized particles. Also Yu et al. [4] investigated several metal and metal oxide nanoparticles in numerous base fluids and found satisfactory results, but many questions concerning these nano-structured material suspensions are still unexplored. In this direction, analyzing the flow dynamics of different nanofluids, Khan et al. [5–10] obtained results that underscored the effectiveness of his study.

Gold nanoparticles play a crucial role in the field of biomedical sciences and shows great potential as effective treatment agents. Gold nanoparticles are currently being studied as drug carriers, photovoltaic agents and contrast agents. Additionally, they are highly regarded as effective compound for drug transfer and delivery due to their ability to encapsulate large amounts of therapeutic molecules. They exhibit several desirable characteristics for cancer therapy. Due to their small size, they can efficiently penetrate various regions of the body, making them suitable for targeted treatment. The utilization of gold nanoparticles allows for the binding of a wide range of proteins and drugs, offering the potential for targeted treatment of cancer cells and elimination of bacteria. The elevated atomic number of these nanoparticles generates heat, making them valuable for selective photothermal therapy in the context of tumor treatment. Xiaohua Huang and Mostafa El-Sayed [11] put forth the optical characteristics and practical uses of gold nanoparticles in the realms of cancer diagnosis and photothermal therapy. Gold nanoparticles have emerged as a focal point of research due to their unique and robust plasmon resonance in the visible spectrum and their applications in the field of biomedical sciences [12]. Researchers have collectively investigated the interaction between gold nanoparticles and blood [13,14].

Tiwari and Das model is also known as homogeneous flow model and has been discussed by Khanfer et al. [15] and is concluded that an enhancement in heat transfer characteristics of nanofluides is only due to the increased thermal conductivity of fluid. This flow model is also known as single phase or single component nanofluid model. Ho et al.[16] did an experiment to see how heat can be moved around in an enclosed space using free convection.They established an improvement of 18% in the heat transport of water with 0.1% of the volume fraction of alumina nanoparticles. The study of the flow of nanofluids using Tiwari and Das model has been done by several researchers [17–28].

In the 19th century, Sophus Lie [29] pioneered the development and application of symmetry groups to differential equations. Lie symmetry groups have found applications in various fields, such as control theory, quantum mechanics, relativity, and mathematical finance. These approaches offer a systematic and mechanical computational algorithm, enabling the explicit determination of the symmetry group for any given system of differential equations. They further employ dimension reduction techniques to optimize the resolution of non-linear differential equations within defined parameter ranges by reducing the order of equations or the number of variables involved. Olver [30] and Bluman and Kumei [31] deliver a comprehensive and thorough treatment of Lie group techniques in the context of differential equations. The advantages of the Lie groups in numerical analysis are extensively discussed in [32–34]

The cone-disk devices have numerous practical and technical applications, such as calculation of viscosity of fluid using viscometry [35], the stability scrutiny of the creeping flow of Oldroyd-B liquid [36], medical purpose [37], applications of bioengineering for propagating endothelium cells placed as a monolayer on the plate [38], for gas turbines in a conical diffuser in the cooling system to compress air [39]. The energy and Navier-Stokes equations for heat transport and laminar flow in cone disk system were originally given by Shevchuk [40] in self-similar versions. Shevchuk demonstrated the compatibility of self-similar solutions with the experimental data provided by Sdougos et al. [41]. Furthermore, Shevchuk showed that the self-similar results are in line with those of Buschmann [42] for smaller conicity. Shevchuk [43] investigated the heat transfer in a conical diffuser and confirmed self-similar solutions with experimental data for a smaller gap angle. Shevchuk [44] extended the analysis of Shevchuk [43] by considering the boundary layer mass transport with the power law radial distribution

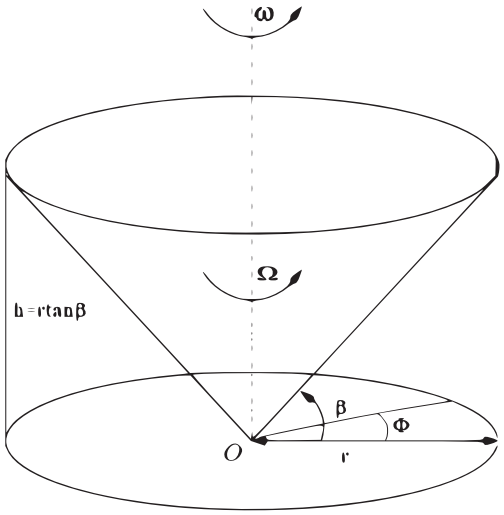


Fig. 1 Physical model

of the concentration at the disk surface. The consideration of heat transfer in rotating disk configuration has gained significant attention in various applications. Von Karman [45] made significant advancements in 1921 by developing similar solutions for symmetrical rotational flow caused by a rotating disk. They highlighted the presence of radially outward flow near the disk surface, which in turn induces an axial inward flow. Batchelor [46] presented a set of equation to analyze the fluid dynamics in the vicinity of a rotating disk, considering the scenario where the surrounding fluid also rotates in the same direction as the disk. Stewartson [47] findings revealed that when using co-rotating discs, the fluid also rotates, whereas in the case if counter-rotating disc, the fluid remains predominantly stationary. Pearson [48] expanded on Stewarson's [47] work by generalizing it time-dependent cases and investigating the fluid dynamics when the disk starts impulsively. Helcig and Shevchuk [49] performed emperical research on the influence of elevated Prandtl numbers (up to 5000) on convective heat transfer, considering temperature-dependent properties. The findings indicated that the observed experimental outcomes align with the self-similar solution proposed by Von karman [45]. Mahanthesh et al. [50] successfully derived self-similar solution for the flow of nanofluids induced by a revolving disk and influenced by surface tension. Dambaru Bhatta and Mahanthesh [51,52] used the Lie group analysis to study the flow and heat transfer of nanofluid in cone-disk system. Turkyilmazoglu [53,54] conducted a comprehensive analysis of the heat transfer occurring in a system with two rotating discs that have ability to expand. Recently flow of different types of nanofluid through cone disk system has been studied by [55–57].

Zafer et al. [58] gave a comprehensive review on the recent development of Tiwari and Das model in nanofluid flow for different geometries. The study of blood carrying gold nanoparticles in cone-disk system has not been explored yet. Such consideration is of great value in biomedical and engineering research as gold nanoparticles play a major role to activate or inhibit the growth of blood vessels. This stems the motivation for the current research which focuses on the gold blood nanofluid flow through cone-disk system in the presence of thermal radiation. The effect of various parameters on four different models of cone-disk system are investigated.

2 Formulation of the problem

A three dimensional steady axisymmetric flow is considered in the cone-disk system, with the assumption that either the cone and disk can either rotate or remain stationary. Here blood is considered as Newtonian fluid which act as base fluid and gold (Au) as nanoparticles. Four configurations are considered namely, model I (a rotating cone with static disk), model II (a rotating disk with static cone), model III (the co-rotation of cone and disk) and model IV (the counter-rotation of cone and disk).

The system is described in cylindrical coordinate with r as radial direction of disk, Φ is azimuthal angle and z is direction perpendicular to the r. Height of cone-disk system is given by $h = r\tan\beta$, where β is the cone angle. The physical model studied in present problem is given in Fig. 1. The rotation speed of cone and disk are given by Ω and ω respectively. The disk is maintained with radially varying temperature $T_\omega(r) = T_\infty + cr^n$, where

c is a positive constant and n is power exponent, it takes positive, zero, or negative values to allow modelling of radially increasing, unvarying, and radially decreasing distribution of T_w on the disk surface [40]. While the surface of the cone is held at a temperature T_∞.
As the flow is axisymmetric, the symmetry is taken in the azimuthal direction, so the derivative with respect to Φ is considered as zero. Under these assumption the governing equations of conservation of mass, conservation of momentum and conservation of energy, taking Rosseland approximation for radiative heat flux into account, are given by [51,59,60]

$$\frac{\partial u_r}{\partial r} + \frac{u_r}{r} + \frac{\partial u_z}{\partial z} = 0, \tag{1}$$

$$\rho_{nf}\left(u_r\frac{\partial u_r}{\partial r} + u_z\frac{\partial u_r}{\partial z} - \frac{u_\Phi^2}{r}\right) = -\frac{\partial p}{\partial r} + \mu_{nf}\left(\frac{\partial^2 u_r}{\partial r^2} + \frac{1}{r}\frac{\partial u_r}{\partial r} - \frac{u_r}{r^2} + \frac{\partial^2 u_r}{\partial z^2}\right), \tag{2}$$

$$\rho_{nf}\left(u_r\frac{\partial u_\Phi}{\partial r} + u_z\frac{\partial u_\Phi}{\partial z} + \frac{u_r u_\Phi}{r}\right) = \mu_{nf}\left(\frac{\partial^2 u_\Phi}{\partial r^2} + \frac{1}{r}\frac{\partial u_\Phi}{\partial r} - \frac{u_\Phi}{r^2} + \frac{\partial^2 u_\Phi}{\partial z^2}\right), \tag{3}$$

$$\rho_{nf}\left(u_r\frac{\partial u_z}{\partial r} + u_z\frac{\partial u_z}{\partial z}\right) = -\frac{\partial p}{\partial z} + \mu_{nf}\left(\frac{\partial^2 u_z}{\partial r^2} + \frac{1}{r}\frac{\partial u_z}{\partial r} + \frac{\partial^2 u_z}{\partial z^2}\right), \tag{4}$$

$$\begin{aligned}(\rho c_p)_{nf}\left(u_r\frac{\partial T}{\partial r} + u_z\frac{\partial T}{\partial z}\right) &= \kappa_{nf}\left(\frac{\partial^2 T}{\partial r^2} + \frac{1}{r}\frac{\partial T}{\partial r} + \frac{\partial^2 T}{\partial z^2}\right)\\ &\quad + \frac{16SbT_\infty^3}{3R_c}\left(\frac{\partial^2 T}{\partial r^2} + \frac{1}{r}\frac{\partial T}{\partial r} + \frac{\partial^2 T}{\partial z^2}\right)\end{aligned} \tag{5}$$

here u_r, u_Φ, u_z are the velocity component in radial, azimuthal and axial direction respectively, p is the pressure, T is temperature. Here radiative heat flux is considered as

$$q_r = -\frac{16SbT_\infty^3}{3R_c}\nabla T. \tag{6}$$

where Sb is the Stefan–Boltzmann constant and R_c is Rosseland mean absorption coefficient. The corresponding boundary conditions are given by [59,60]:

$$u_r = 0,\ u_\Phi = \omega r,\ u_z = 0,\ T = T_\omega(r) \text{ at } z = 0 \text{ (at disk)}, \tag{7}$$

$$u_r = 0,\ u_\Phi = \Omega r,\ u_z = 0,\ T = T_\infty \text{ at } z = h \text{ (at cone)}, \tag{8}$$

The effective dynamic viscosity μ_{nf}, The effective density ρ_{nf}, the effective heat capacity $(\rho c_p)_{nf}$ and the effective thermal conductivity κ_{nf} of nanofluid are defined as [61]:

$$\begin{aligned}\mu_{nf} &= \frac{\mu_f}{(1-\phi)^{2.5}};\\ \rho_{nf} &= (1-\phi)\rho_f + \phi\rho_s;\\ (\rho c_p)_{nf} &= (1-\phi)(\rho c_p)_f + \phi(\rho c_p)_s;\\ \frac{\kappa_{nf}}{\kappa_f} &= \frac{\kappa_s + 2\kappa_f - 2\phi(\kappa_f - \kappa_s)}{\kappa_s + 2\kappa_f + \phi(\kappa_f - \kappa_s)};\end{aligned} \tag{9}$$

where ρ_f pertains to the density of the base fluid, ρ_s is associated with the density of the nanoparticles, while ϕ quantifies the volume fraction of nanoparticles. In addition, $(\rho c_p)_f$, $(\rho c_p)_s$ correspond to the heat capacitance of the base fluid and nanoparticles, respectively, and κ_f, κ_s are used to specify the thermal conductivity of the base fluid and nanoparticles.

The thermophysical properties of blood and gold nanoparticles are given in the Table 1:

Table 1 Thermophysical properties of blood and gold nanoparticles [62]

Material	Density(ρ) (kg/m^3)	Specific heat (c_p) (J/kgK)	Thermal conductivity (κ) (W/mK)	Dynamic viscosity (μ) ($Pa.s$)
Blood	$\rho_f = 1063$	$(c_p)_f = 3617$	$\kappa_f = 0.52$	$\mu_f = 0.003$
Gold(Au)	$\rho_s = 19300$	$(c_p)_s = 129$	$\kappa_s = 318$	$\mu_s = 0.00464$

3 Lie group analysis

The systematic utilization of Lie symmetry group analysis allows for the derivation of invariant similarity transformations that, in turn, lead to ordinary differential equations from the governing partial differential equations. Consider the following transformation of the Lie Group [30,63];

$$\Gamma: \begin{cases} r^* = re^{\epsilon b_1}, z^* = ze^{\epsilon b_2}, u_r^* = u_r e^{\epsilon b_3}, \\ u_\Phi^* = u_\Phi e^{\epsilon b_4}, u_z^* = u_z e^{\epsilon b_5}, p^* = pe^{\epsilon b_6}. \end{cases} \tag{10}$$

here ϵ is the parameter of lie group and $b_i (i = 1, 2, ...6)$ are arbitrary real constant to be determined under invariant conditions. Using Eq. (10) in Eqs. (1)–(4), following new relations are obtained

$$b_3 - b_1 = b_5 - b_2, \tag{11}$$
$$2b_3 - b_1 = b_5 + b_3 - b_2 = 2b_4 - b_1 = b_6 - b_1 = b_3 - 2b_1 = b_3 - 2b_2, \tag{12}$$
$$b_3 + b_4 - b_1 = b_5 + b_4 - b_2 = b_4 - 2b_1 = b_4 - 2b_2, \tag{13}$$
$$b_3 + b_5 - b_1 = 2b_5 - b_2 = b_6 - b_2 = b_5 - 2b_1 = b_5 - 2b_2. \tag{14}$$

Solving Eqs. (11)–(14) following relations are obtained

$$b_2 = b_1, b_3 = b_4 = b_5 = -b_1, b_6 = -2b_1. \tag{15}$$

Substituting the value of Eq. (15) into Eq. (10), transformation of Lie group becomes

$$\Gamma: \begin{cases} r^* = re^{\epsilon b_1}, z^* = ze^{\epsilon b_1}, u_r^* = u_r e^{-\epsilon b_1}, \\ u_\Phi^* = u_\Phi e^{-\epsilon b_1}, u_z^* = u_z e^{-\epsilon b_1}, p^* = pe^{-2\epsilon b_1}. \end{cases} \tag{16}$$

Using derivation process [59] in Eq. (16), following characteristics equations are obtained

$$\frac{dr}{r} = \frac{dz}{z} = \frac{du_r}{-u_r} = \frac{du_\Phi}{-u_\Phi} = \frac{du_z}{-u_z} = \frac{dp}{-2p} \tag{17}$$

After solving and normalizing (17), following similarity transformation are obtained

$$\begin{aligned} &\eta = \frac{z}{r}, F(\eta) = \frac{r}{\upsilon_f} u_r, G(\eta) = \frac{r}{\upsilon_f} u_\Phi, \\ &H(\eta) = \frac{r}{\upsilon_f} u_z, P(\eta) = \frac{pr^2}{\rho_f \upsilon_f^2}, \theta(\eta) = \frac{T - T_\infty}{T_w - T_\infty}, \end{aligned} \tag{18}$$

here the terms η, F, G, H, P, and θ correspond to dimensionless similarity variable, radial velocity, azimuthal velocity, axial velocity, pressure, and temperature, respectively.

Table 2 Comparison for the value of Nu_d with the data in Turkyilmazoglu [60] and Basavarajappa [51] when $Re = 12$, $Rd = 0$ and $Pr = 0.71$ for $\beta = \pi/4$

		Turkyilmazoglu [60] (Runge-Kutta method)	Basavarajappa [51]	Present Results
Model I	$n = -1$	1.17660019	1.17660024	1.17660043
	$n = 0$	1.09328442	1.09328437	1.09328437
	$n = 2$	−1.54423530	−1.54422303	−1.54421437
Model II	$n = -1$	1.09783630	1.09783626	1.09783624
	$n = 0$	1.17198527	1.17198529	1.17198533
	$n = 2$	−0.93598578	−0.93596154	−0.93599083
Model III	$n = -1$	1.13380335	1.13379245	1.13380343
	$n = 0$	1.13538224	1.13540222	1.13538216
	$n = 2$	−1.18400733	−1.18388642	−1.18400793
Model IV	$n = -1$	1.14297867	1.14297868	1.14297867
	$n = 0$	1.12618149	1.12618149	1.12618150
	$n = 2$	−1.33449962	−1.33449993	−1.33449161

Table 3 Comparison for the value of Nu_c with the data in Turkyilmazoglu [60] and Basavarajappa [51] when $Re = 12$, $Rd = 0$ and $Pr = 0.71$ for $\beta = \pi/4$

		Turkyilmazoglu [60] (Runge-Kutta method)	Basavarajappa [51]	Present Results
Model I	$n = -1$	0.58830009	0.58830012	0.58830021
	$n = 0$	0.83028093	0.83028103	0.83028103
	$n = 2$	3.47605658	3.47604646	3.47604668
Model II	$n = -1$	0.54891815	0.54891813	0.5489182
	$n = 0$	0.78069847	0.78069848	0.78069843
	$n = 2$	3.34300860	3.34296550	3.34300751
Model III	$n = -1$	0.56690167	0.56689626	0.56690171
	$n = 0$	0.80178312	0.80177021	0.80178317
	$n = 2$	3.36462622	3.36460059	3.36462635
Model IV	$n = -1$	0.57148934	0.57148934	0.57148934
	$n = 0$	0.81339331	0.81339331	0.81339331
	$n = 2$	3.50319972	3.50320003	3.50319131

4 Self-similar equations

On employing self similar transformation (18) in the governing Eqs. (1) to (4), the transformed ordinary differential equations are:

$$H' - \eta F' = 0, \tag{19}$$

$$A(1+\eta^2)F'' + \{3A\eta + B(\eta F - H)\}F' + B(F^2 + G^2) + 2P + \eta P' = 0, \tag{20}$$

$$A(1+\eta^2)G'' + \{3A\eta + B(\eta F - H)\}G' = 0 \tag{21}$$

$$A(1+\eta^2)H'' + \{3A\eta + B(\eta F - H)\}H' + (A + BF)H - P' = 0 \tag{22}$$

$$\frac{C + Rd}{PrD}\{(1+\eta^2)\theta'' + \eta(1-2n)\theta' + n^2\theta\} + (\eta F - H)\theta' - nF\theta = 0 \tag{23}$$

where $'$ denotes the derivative with respect to η. The boundary conditions (7)-(8), after using self similar transformation (18) become

$$F(\eta) = 0,\ G(\eta) = Re_\omega,\ H(\eta) = 0,\ \theta(\eta) = 1 \text{ at } \eta = 0, \tag{24}$$

$$F(\eta) = 0,\ G(\eta) = Re_\Omega,\ H(\eta) = 0,\ \theta(\eta) = 0 \text{ at } \eta = tan(\beta), \tag{25}$$

$$\text{here} \quad A = \frac{\mu_{nf}}{\mu_f},\ B = \frac{\rho_{nf}}{\rho_f},\ C = \frac{\kappa_{nf}}{\kappa_f},\ \text{and } D = \frac{(\rho c_p)_{nf}}{(\rho c_p)_f} \tag{26}$$

are nanofluid property ratios. The dimensionless parameters that involved in above equations are:

- The Prandtl number ($Pr = \frac{\rho_f c_{pf} \upsilon_f}{\kappa_f}$) quantifies the relative importance of the base fluid's kinematic viscosity and thermal diffusivity. In this particular investigation, $Pr = 21$ is taken, aligning with the properties of blood.
- The Rosseland radiation parameter, denoted as $Rd = \frac{16SbT_\infty^3}{3R_c\kappa_f}$, is employed to assess the impact of thermal radiation and is characterized by positive values.
- Rotational Reynolds numbers, denoted as $Re_\omega = \frac{\omega r^2}{\upsilon_f}$ and $Re_\Omega = \frac{\Omega r^2}{\upsilon_f}$, are defined based on the angular velocities, ω and Ω, associated with the disk and cone respectively. Following Shevchuck's [59] approach, the rotational Reynolds numbers are selected as 12, corresponding to gap angles of 45°, which represents a relatively large gap.

After eliminating the pressure term from Eqs. (20) and (22), following equation is obtained

$$\begin{aligned} A(1+\eta^2)^2F''' + (1+\eta^2)\{10A\eta + B(\eta F - H)\}F'' + \\ 3F'\{A(2+7\eta^2) + B(1+2\eta^2)F - B\eta H\} \\ + 2BGG' + 3(A+BF)H = 0 \end{aligned} \tag{27}$$

Therefore, Eqs. (19), (21) and (27) are to be solved for velocity components. The pressure field can be obtained by integrating Eq. (22) and is given by

$$P = \eta A(1+\eta^2)F' + \eta(A+BF)H - BH^2 + \Pi^2$$

where Π is the constant of integration.

5 Implementation of bvp5c solver

The nonlinear differential Eqs. (19), (21), (23) and (27) are solved numerically together with boundary conditions (24) and (25), using bvp5c solver of MATLAB for different values of flow parameter. In order to apply bvp5c [64] solver, the nonlinear differential equations must be written as a system of first-order ordinary differential equations. Introducing the following new variables,

$$f(1) = F,\ f(2) = F',\ f(3) = F'',\ f(4) = H$$

$$f(5) = G,\ f(6) = G',\ f(7) = \theta,\ f(8) = \theta'$$

Putting these new variables into the Eqs. (19), (21), (23) and (27), the new system of first order equations are obtained

$$f'(1) = f(2),$$

$$f'(2) = f(3),$$

$$\begin{aligned} f'(3) = \frac{1}{A(1+\eta^2)^2}\Big\{ & -(1+\eta^2)[10\eta A + B(\eta f(1) - f(4))]f(3) - 2Bf(5)f(6) \\ & - 3f(2)[A(2+7\eta^2) + B(1+2\eta^2)f(1) - \eta Bf(4)] - 3[A + Bf(1)]f(4)\Big\}, \end{aligned}$$

$$f'(4) = \eta f(2),$$

$$f'(5) = f(6),$$

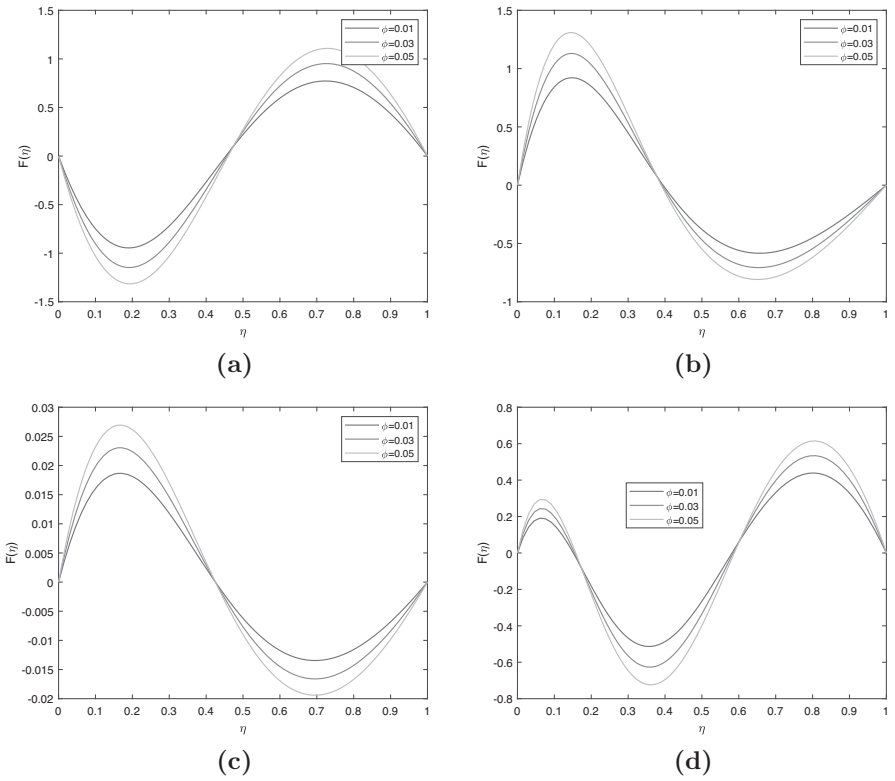


Fig. 2 Effect of ϕ on radial velocity profile $F(\eta)$ for gold blood nanofluid for **a** stationary disk and rotating cone **b** rotating disk and stationary cone **c** co-rotation of disk and cone **d** counter rotation of disk and cone

$$f'(6) = \frac{-1}{A(1+\eta^2)}\Big\{3\eta A f(6) + B[\eta f(1) - f(4)]f(6)\Big\},$$

$$f'(7) = f(8),$$

$$f'(8) = \frac{1}{1+\eta^2}\left\{\frac{PrD}{Rd+C}[(f(4) - \eta f(1))f(8) + nf(1)f(7)] - \eta(1-2n)f(8) - n^2 f(7)\right\}.$$

The boundary conditions after using new variables are:

$$f_a(1) = 0,\ \ f_a(5) = Re_\omega,\ \ f_a(4) = 0,\ \ f_a(7) = 1$$

$$f_b(1) = 0,\ \ f_b(5) = Re_\Omega,\ \ f_b(4) = 0,\ \ f_b(7) = 0$$

here, f_a denotes the positions of $\eta = 0$ and f_b denotes the positions of $\eta = tan(\beta)$.

6 Result and discussion

System of equation given by (19), (21) (23) and (27) along with boundary condition, (24) and (25) is simulated numerically with the help of bvp5c solver of MATLAB to find the velocity and temperature profiles for the cone-disk system corresponding to four different configurations. Here the value of rotational Reynolds number is taken 12, which corresponding to the gap angle 45° [59]. The value of Prandtl number is set 21 which corresponding to blood, which act here as base fluid. To validate the result a comparison is performed with available published data. The value of the Nusselt number at the disk and cone are compared with those of Turkyilmazoglu [60] and

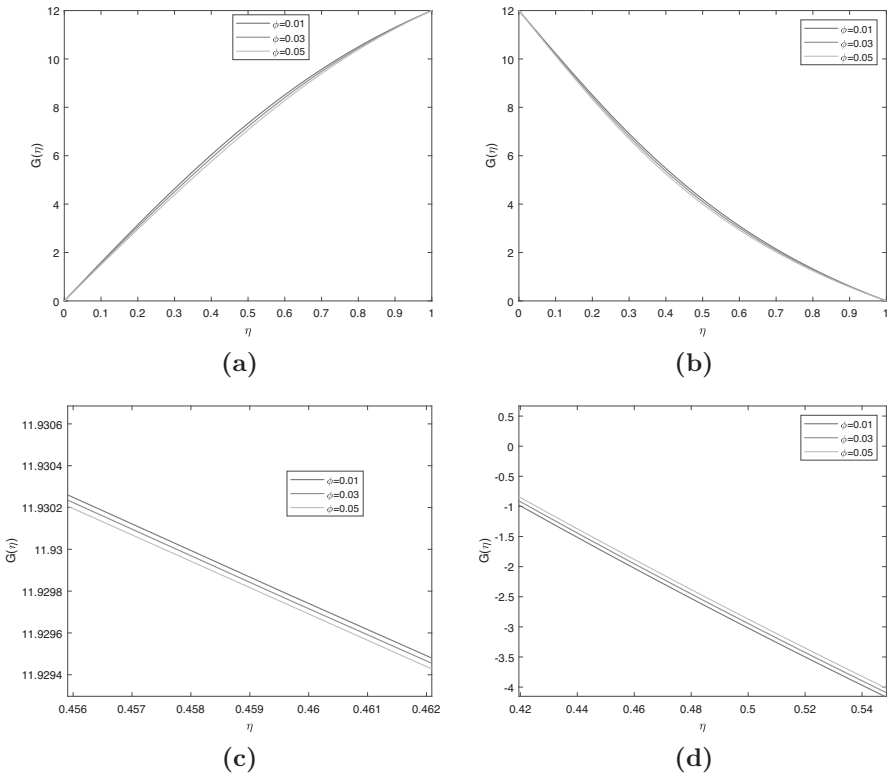


Fig. 3 Effect of ϕ on azimuthal velocity profile $G(\eta)$ for gold blood nanofluid for **a** stationary disk and rotating cone **b** rotating disk and stationary cone **c** co-rotation of disk and cone **d** counter rotation of disk and cone

Basavarajappa [51] and is given in Table 2 and Table 3. The closed agreement authenticates validation of the problem.

The nanofluid flow velocity components in radial $F(\eta)$, azimuthal $G(\eta)$ and axial $H(\eta)$ direction are presented in Figs. 2–4 for the gap angle $\pi/4$. In case of stationary disk and rotating cone (model I) radial velocity component $F(\eta)$ behave radially inward near the disk surface and radially outward near the cone surface. As the cone is rotating, so near the cone surface centrifugal force is high, due to which there is an outward radial flow near the cone. In case of rotating disk and stationary cone (model II) radial velocity behave opposite to that of model I. As the disk is rotating and the centrifugal force give rise to outward flow near the disk. In the case of co-rotating disk and cone (model III) the value of rotational Reynolds number are takes as $Re_\omega = 12$ and $Re_\Omega = 11.8812$ i.e. $Re_\omega > Re_\Omega$. In this case the radial velocity behave similar to that of model II. If $Re_\omega < Re_\Omega$ the the radial velocity behave like model I, but the magnitude of velocity remains smaller. In model IV, where the disk and cone rotate in opposite directions, here the values of $Re_\omega = 12$ and $Re_\Omega = -12$ is taken corresponding to disk and cone. Due to counter rotation of disk and cone there is outward flow near both the surfaces and the radial velocity $F(\eta)$ changes its sign twice. Figure 3 shows the variation of Tangential velocity $G(\eta)$ and it is observed that it behave linearly for all the four configuration of cone-disk system. Figure 4 shows the behaviour of axial velocity $H(\eta)$ w.r.t. η. It is interpreted from the figure that the axial velocity behave in similar way for model I and model IV and an opposite trend is observed for model II and III. These results are in good agreement with Shevchuk [59] and Basavarajappa [51].

The variation of radial, tangential and axial velocity with the nanoparticle volume fraction parameter for all the four configuration are shown in Figs. 2 – 4. Figure 2a–d gives the graphical representation of the radial velocity $F(\eta)$ for different values of ϕ for all four models. Figure 2a shows the graphical variation of radial velocity for different value of nanoparticle volume fraction parameter for model I. It is found that with an increase in the value of ϕ, velocity decrease near the stationary disk surface, it is because as ϕ increases the density of fluid increases which causes decrease in the velocity, but the radial velocity increases near the rotating cone due to the centrifugal forces. In case of rotating disk and stationary cone (model II) velocity increases with an increase

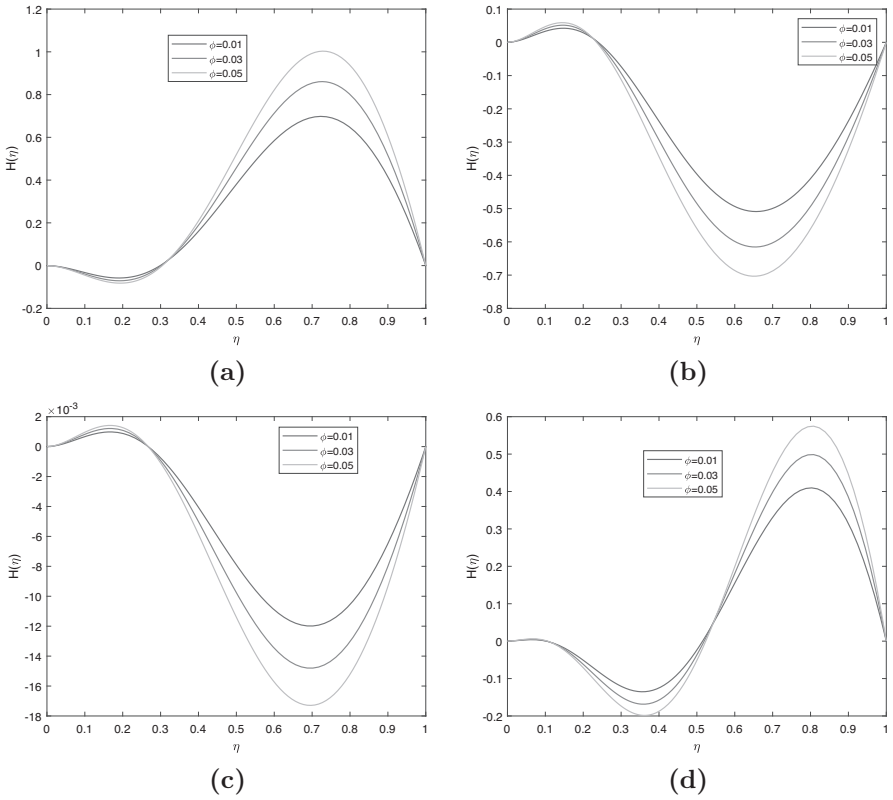


Fig. 4 Effect of ϕ on axial velocity profile $H(\eta)$ for gold blood nanofluid for **a** stationary disk and rotating cone **b** rotating disk and stationary cone **c** co-rotation of disk and cone **d** counter rotation of disk and cone

in the value of ϕ near rotating cone, but then it decreases in the region near the stationary cone and is shown in Fig. 2b, which is exactly opposite to model I. Same trend of radial velocity is seen for the co-rotating disk and cone (model III) but the magnitude of velocity is less and is given in Fig. 2c. When the disk and cone are rotating in opposite direction the variation of radial velocity with ϕ is shown in Fig. 2d. From the figure it is interpreted that velocity increases near the disk surface, then it decreases and again it increases near the region of rotating cone. It is also observed that magnitude of velocity is more near the cone as compare to the disk surface.

Figure 3a–d shows the effect of nanoparticle volume fraction on the tangential velocity $G(\eta)$ for four different configuration. Figure 3a shows the effect of ϕ on velocity for stationary disk and rotating cone (model I) and it is observed that with increase in ϕ velocity decreases and the magnitude of velocity increases in the region near the rotating cone. As excepted the opposite trend is seen for rotating disk and stationary cone (model II), here magnitude of velocity is high at rotating disk surface and it is shown in Fig. 3b. It is observed that velocity decreases with increase in ϕ for co-rotation of disk and cone as shown in Fig. 3c. Figure 3d shows that velocity increases with ϕ for counter rotation of disk and cone.

The effect of ϕ on axial velocity $H(\eta)$ four for all models are shown in Fig. 4a–d. There is decrease in axial velocity near the stationary disk but it increases near the rotating cone as the value of ϕ increases and is shown in Fig. 4a. From Fig. 4b it is observed that there is very small increase in velocity near rotating disk but the velocity decreases significantly near the stationary cone. Same trend of axial velocity is observed for model III but the magnitude of velocity is different and is shown in Fig. 4c. It is observed from Fig. 4d that axial velocity decreases with increase in ϕ near the rotating disk but then it increases near the rotating cone. This pattern is same as that of model I but the magnitude of velocity is different.

The variation of temperature with ϕ for four different configuration of cone and disk are shown in Fig. 5a–d. Figure 5a shows the variation of temperature profile for stationary disk and rotating cone (model I) and its found that temperature increases with increases in ϕ, as with increase in nanoparticle volume fraction parameter ϕ, the fluid become denser, resulting an increasing in temperature profile. Same trend is observed for counter rotation of

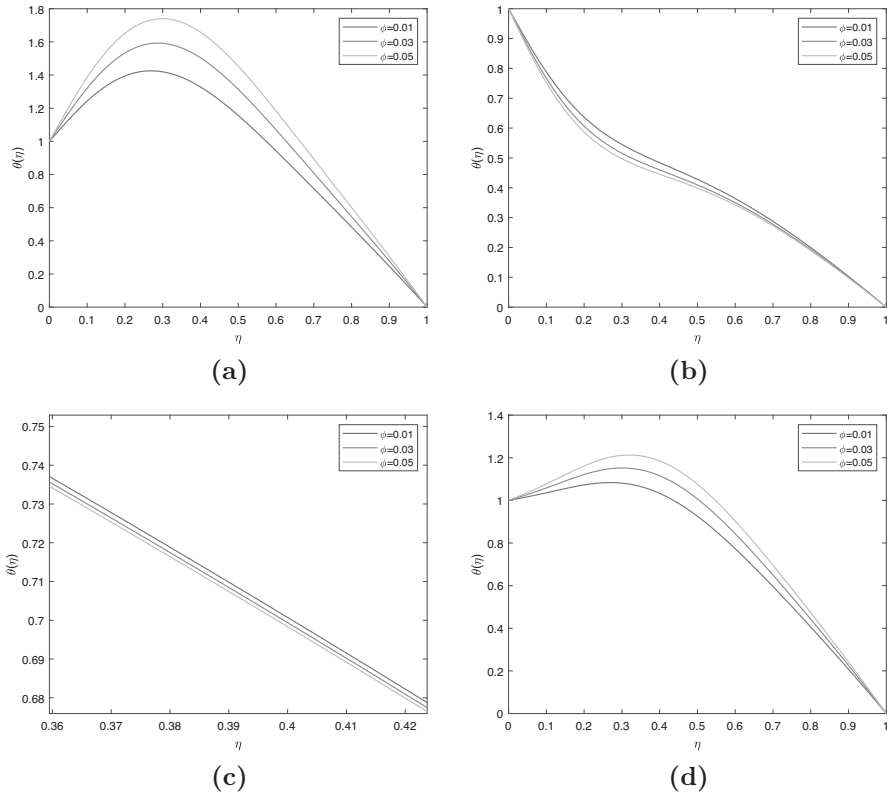


Fig. 5 Effect of ϕ on temperature profile $\theta(\eta)$ for gold blood nanofluid for **a** stationary disk and rotating cone **b** rotating disk and stationary cone **c** co-rotation of disk and cone **d** counter rotation of disk and cone, for $Pr = 21$, $Rd = 1$, and $n = 1$.

disk and cone and is shown in Fig. 5d. Figure 5b and c shows that temperature profile decreases with an increase in the value of ϕ which corresponds to model II and model III.

The variation of temperature for the different values of power exponent n is represented in Fig. 6a–d. Negative value of n mean radially diminishing disk surface, $n = 0$ means unvarying disk surface and positive value of n corresponds to radially increasing disk surface. From the Fig. 6, it can be seen that $\theta(\eta)$ reduce from unit value at disk to zero values at cone. Figure 6a shows that the temperature profile increases with increasing value of n and this increase in temperature is more prominent near the disk surface than the cone (model I). Figure 6b show the results for model II. From the figure it is clear that temperature profile decrease near the disk whereas it increase near the cone. Temperature field increase with the increase of n for both III and IV model. Variation of temperature profile is in good agreement with that of Shevchuk [59], Turkyilmozoglu [60] and Basavarajappa [51]. Variation of radiation parameter on temperature profile has been shown in Fig. 7a–d for all four model. From the graph it is seen that with the increase in radiation parameter temperature profile decrease for I and IV model, as expected radiation decreases the rate of energy transported to fluid and hence decrease in the fluid temperature, whereas an opposite trend is observed for model II and model III.

7 Conclusion

In this paper velocity and temperature gold blood nanofluid in cone-disk system in the presence of thermal radiation has been analysed using lie group approach. Here blood is considered as Newtonian fluid. Present problem is important due to its applications in targeted drug delivery system and medical devices. The gold particles are efficient drug-carrying and drug-delivery vechiles as they can encapsulate large quantity of therapeutic molecules. The effect of different parameters on velocity and temperature profile has been discussed. It is concluded that:

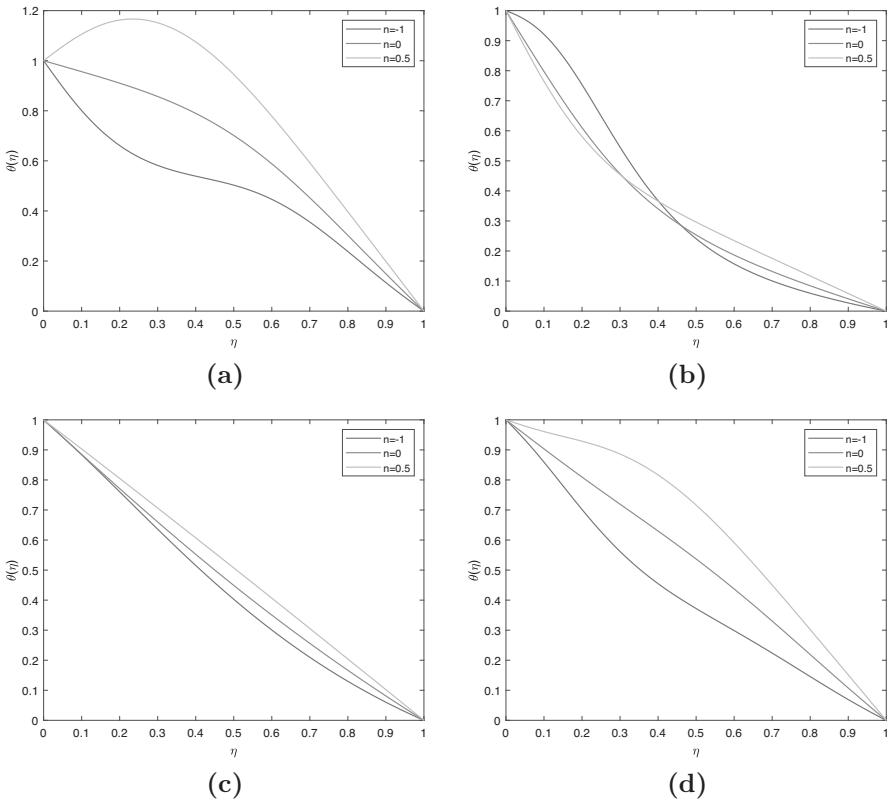


Fig. 6 Effect of n on temperature profile $\theta(\eta)$ for gold blood nanofluid for **a** stationary disk and rotating cone **b** rotating disk and stationary cone **c** co-rotation of disk and cone **d** counter rotation of disk and cone, for $Pr = 21$, $Rd = 1$ and $\phi = 0.05$

- Velocity of gold blood nanofluid increases near the rotating disk/cone, due to high centrifugal force in that region.
- Velocity of blood nanofluid decreases with increasing value of nanopartical volume fraction parameter ϕ, it is because as ϕ increases the density of fluid increases which causes decrease in the velocity.
- The temperature profile of gold blood nanofluid increases with increases in nanopartical volume fraction parameter ϕ as with addition of nanoparticle to base fluid the denser behaviour of fluid enhanced which results an increase in temperature profile.
- The temperature profile of gold blood nanofluid increases with increase in power index n for I, III and IV model whereas for model II it decreases near the disk then increases near the cone.
- The velocity and temperature profile are in good agreement with Shevchuk [59].
- The result for present problem can be validated by comparing the heat transfer rate at cone and disk that of Turkyilmazoglu [60] and Basavarajappa [51] for $Re = 12$, $Rd = 0$, $Pr = 0.71$ for $\beta = \pi/4$

8 Future Suggestions

- The same model could be extended to the unsteady case.
- The researcher can use slip an jump conditions for the same model.

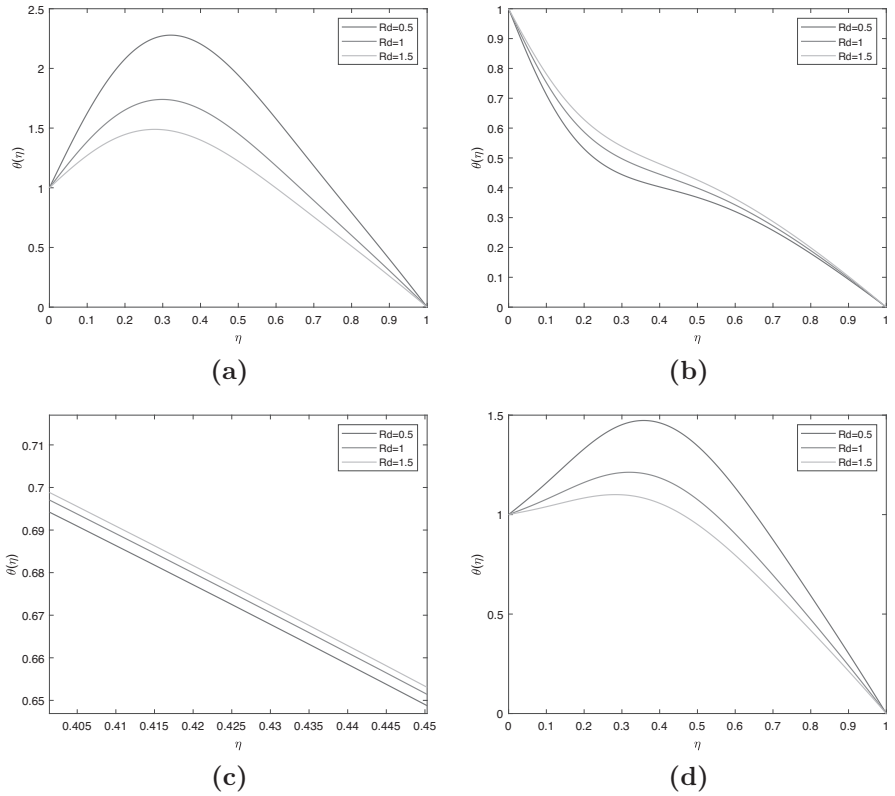


Fig. 7 Effect of Rd on temperature profile $\theta(\eta)$ for gold blood nanofluid for **a** stationary disk and rotating cone **b** rotating disk and stationary cone **c** co-rotation of disk and cone **d** counter rotation of disk and cone, for $Pr = 21$, $n = 1$ and $\phi = 0.05$

Acknowledgements Authors are grateful to the reviewer for his valuable suggestions for the improvement of manuscript. One of the author gratefully acknowledge the financial assistance given by National Fellowship for Backward Classes Students (NFOBC) New Delhi.

Declarations

Competing interest There are no relevant financial or non-financial competing interests to report.

References

1. Sheikhpour, M., Arabi, M., Kasaeian, A., Rokn Rabei, A., Taherian, Z.: Role of nanofluids in drug delivery and biomedical technology: Methods and applications. Nanotechnology, Science and Applications, 47–59 (2020) https://doi.org/10.2147/NSA.S260374
2. Choi, S.U.S., Eastman, J.A.: Enhancing thermal conductivity of fluids with nanoparticles (1995)
3. Choi, S.U.: Nanofluids: from vision to reality through research (2009) https://doi.org/10.1115/1.3056479
4. Yu, W., France, D.M., Routbort, J.L., Choi, S.U.: Review and comparison of nanofluid thermal conductivity and heat transfer enhancements. Heat transfer engineering 29(5), 432–460 (2008) https://doi.org/10.1080/01457630701850851
5. Khan, A., Shah, Z., Alzahrani, E., Islam, S.: Entropy generation and thermal analysis for rotary motion of hydromagnetic casson nanofluid past a rotating cylinder with joule heating effect. International Communications in Heat and Mass Transfer 119, 104979 (2020) https://doi.org/10.1016/j.icheatmasstransfer.2020.104979
6. Khan, A., Saeed, A., Gul, T., Mukhtar, S., Ali, I., Jawad, M.: Radiative swirl motion of hydromagnetic casson nanofluid flow over rotary cylinder using joule dissipation impact. Physica Scripta 96(4), 045206 (2021) https://doi.org/10.1088/1402-4896/abdf83
7. Khan, A., Saeed, A., Tassaddiq, A., Gul, T., Kumam, P., Ali, I., Kumam, W.: Bio-convective and chemically reactive hybrid nanofluid flow upon a thin stirring needle with viscous dissipation. Scientific reports 11(1), 8066 (2021) https://doi.org/10.1038/s41598-021-86968-8
8. Khan, A., Saeed, A., Tassaddiq, A., Gul, T., Mukhtar, S., Kumam, P., Ali, I., Kumam, W.: Bio-convective micropolar nanofluid flow over thin moving needle subject to arrhenius activation energy, viscous dissipation and binary chemical reaction. Case Studies in Thermal Engineering 25, 100989 (2021) https://doi.org/10.1016/j.csite.2021.100989

9. Khan, A., Kumam, W., Khan, I., Saeed, A., Gul, T., Kumam, P., Ali, I.: Chemically reactive nanofluid flow past a thin moving needle with viscous dissipation, magnetic effects and hall current. Plos one 16(4), 0249264 (2021) https://doi.org/10.1371/journal.pone.0249264
10. Islam, S., Khan, A., Kumam, P., Alrabaiah, H., Shah, Z., Khan, W., Zubair, M., Jawad, M.: Radiative mixed convection flow of maxwell nanofluid over a stretching cylinder with joule heating and heat source/sink effects. Scientific reports 10(1), 17823 (2020) https://doi.org/10.1038/s41598-020-74393-2
11. Huang, X., El-Sayed, M.A.: Gold nanoparticles: Optical properties and implementations in cancer diagnosis and photothermal therapy. Journal of advanced research 1(1), 13–28 (2010) https://doi.org/10.1016/j.jare.2010.02.002
12. Kumar, K.P., Paul, W., Sharma, C.P.: Green synthesis of gold nanoparticles with zingiber officinale extract: characterization and blood compatibility. Process Biochemistry 46(10), 2007–2013 (2011) https://doi.org/10.1016/j.procbio.2011.07.011
13. Hatami, M., Hatami, J., Ganji, D.D.: Computer simulation of mhd blood conveying gold nanoparticles as a third grade non-newtonian nanofluid in a hollow porous vessel. Computer methods and programs in biomedicine 113(2), 632–641 (2014) https://doi.org/10.1016/j.cmpb.2013.11.001
14. Rahbari, A., Fakour, M., Hamzehnezhad, A., Vakilabadi, M.A., Ganji, D.: Heat transfer and fluid flow of blood with nanoparticles through porous vessels in a magnetic field: A quasi-one dimensional analytical approach. Mathematical biosciences 283, 38–47 (2017) https://doi.org/10.1016/j.mbs.2016.11.009
15. Khanafer, K., Vafai, K., Lightstone, M.: Buoyancy-driven heat transfer enhancement in a two-dimensional enclosure utilizing nanofluids. International journal of heat and mass transfer 46(19), 3639–3653 (2003) https://doi.org/10.1016/S0017-9310(03)00156-X
16. Ho, C., Liu, W., Chang, Y., Lin, C.: Natural convection heat transfer of alumina-water nanofluid in vertical square enclosures: An experimental study. International Journal of Thermal Sciences 49(8), 1345–1353 (2010) https://doi.org/10.1016/j.ijthermalsci.2010.02.013
17. Sheremet, M.A., Grosan, T., Pop, I.: Free convection in a square cavity filled with a porous medium saturated by nanofluid using tiwari and das' nanofluid model. Transport in Porous Media 106, 595–610 (2015) https://doi.org/10.1007/s11242-014-0415-3
18. Rashad, A.M., Gorla, R.S.R., Mansour, M., Ahmed, S.E.: Magnetohydrodynamic effect on natural convection in a cavity filled with a porous medium saturated with nanofluid. Journal of Porous Media 20(4) (2017) https://doi.org/10.1615/JPorMedia.v20.i4.50
19. Selimefendigil, F., Öztop, H.F., Chamkha, A.J.: Mhd mixed convection and entropy generation of nanofluid filled lid driven cavity under the influence of inclined magnetic fields imposed to its upper and lower diagonal triangular domains. Journal of Magnetism and Magnetic Materials 406, 266–281 (2016) https://doi.org/10.1016/j.jmmm.2016.01.039
20. Sheikholeslami, M.: Influence of magnetic field on nanofluid free convection in an open porous cavity by means of lattice boltzmann method. Journal of Molecular Liquids 234, 364–374 (2017) https://doi.org/10.1016/j.molliq.2017.03.104
21. Rashad, A., Rashidi, M., Lorenzini, G., Ahmed, S.E., Aly, A.M.: Magnetic field and internal heat generation effects on the free convection in a rectangular cavity filled with a porous medium saturated with cu–water nanofluid. International Journal of Heat and Mass Transfer 104, 878–889 (2017) https://doi.org/10.1016/j.ijheatmasstransfer.2016.08.025
22. Ghasemi, K., Siavashi, M.: Lattice boltzmann numerical simulation and entropy generation analysis of natural convection of nanofluid in a porous cavity with different linear temperature distributions on side walls. Journal of Molecular Liquids 233, 415–430 (2017) https://doi.org/10.1016/j.molliq.2017.03.016
23. Sheikholeslami, M.: Influence of magnetic field on al2o3-h2o nanofluid forced convection heat transfer in a porous lid driven cavity with hot sphere obstacle by means of lbm. Journal of Molecular Liquids 263, 472–488 (2018) https://doi.org/10.1016/j.molliq.2018.04.111
24. Basak, T., Chamkha, A.J.: Heatline analysis on natural convection for nanofluids confined within square cavities with various thermal boundary conditions. International Journal of Heat and Mass Transfer 55(21-22), 5526–5543 (2012) https://doi.org/10.1016/j.ijheatmasstransfer.2012.05.025
25. Mehryan, S., Izadi, M., Sheremet, M.A.: Analysis of conjugate natural convection within a porous square enclosure occupied with micropolar nanofluid using local thermal non-equilibrium model. Journal of Molecular Liquids 250, 353–368 (2018) https://doi.org/10.1016/j.molliq.2017.11.177
26. Zhou, Y., Rajapakse, R., Graham, J.: Coupled consolidation of a porous medium with a cylindrical or a spherical cavity. International Journal for Numerical and Analytical Methods in Geomechanics 22(6), 449–475 (1998) https://doi.org/10.1002/(SICI)1096-9853(199806)22:6<449::AID-NAG930>3.0.CO;2-H
27. Toosi, M.H., Siavashi, M.: Two-phase mixture numerical simulation of natural convection of nanofluid flow in a cavity partially filled with porous media to enhance heat transfer. Journal of Molecular Liquids 238, 553–569 (2017) https://doi.org/10.1016/j.molliq.2017.05.015
28. Sivasankaran, S., Mansour, M., Rashad, A., Bhuvaneswari, M.: Mhd mixed convection of cu–water nanofluid in a two-sided lid-driven porous cavity with a partial slip. Numerical Heat Transfer, Part A: Applications 70(12), 1356–1370 (2016) https://doi.org/10.1080/10407782.2016.1243957
29. Lie, S.: Über die integration durch bestimmte integrale von einer classe linearer partieller differentialgleichungen (1880)
30. Olver, P.J.: Applications of lie groups to differential equations (1993)
31. Bluman, G.W., Kumei, S.: Symmetries and differential equations 81 (2013)
32. Gröbner, W., Knapp, H.: Contributions to the method of lie series 802 (1967)
33. Shokin, I.I., Ianenko, N.: The method of differential approximation: application to gas dynamics. Novosibirsk Izdatel Nauka (1985)
34. Dorodnitsyn, V.: Transformation groups in net spaces. Journal of Soviet mathematics 55, 1490–1517 (1991) https://doi.org/10.1007/BF01097535
35. Mooney, M., Ewart, R.: The conicylindrical viscometer. Physics 5(11), 350–354 (1934) https://doi.org/10.1063/1.1745219
36. Phan-Thien, N.: Cone-and-plate flow of the oldroyd-b fluid is unstable. Journal of non-newtonian fluid mechanics 17(1), 37–44 (1985) https://doi.org/10.1016/0377-0257(85)80004-5

37. Spruell, C., Baker, A.B.: Analysis of a high-throughput cone-and-plate apparatus for the application of defined spatiotemporal flow to cultured cells. Biotechnology and bioengineering 110(6), 1782–1793 (2013) https://doi.org/10.1002/bit.24823
38. Buschmann, M., Dieterich, P., Adams, N., Schnittler, H.-J.: Analysis of flow in a cone-and-plate apparatus with respect to spatial and temporal effects on endothelial cells. Biotechnology and bioengineering 89(5), 493–502 (2005) https://doi.org/10.1002/bit.20165
39. Owen, J.M.: Flow and heat transfer in rotating-disc systems. In: International Symposium on Heat Transfer in Turbomachinery (1992). https://doi.org/10.1615/ICHMT.1994.IntSympHetatTransTurb . Begel House Inc.
40. Shevchuk, I.: A self-similar solution of navier–stokes and energy equations for rotating flows between a cone and a disk. High temperature 42(1), 104–110 (2004) https://doi.org/10.1023/B:HITE.0000020097.59838.02
41. Sdougos, H., Bussolari, S., Dewey, C.: Secondary flow and turbulence in a cone-and-plate device. Journal of Fluid Mechanics 138 (1984) https://doi.org/10.1017/S0022112084000161
42. Buschmann, M.H.: A solution for the flow between a cone and a plate at low reynolds number. Journal of Thermal Science 11, 289–295 (2002) https://doi.org/10.1007/s11630-002-0041-1
43. Shevchuk, I.: Laminar heat transfer of a swirled flow in a conical diffuser. self-similar solution. Fluid Dynamics 39(1), 42–46 (2004) https://doi.org/10.1023/B:FLUI.0000024810.83169.57
44. Shevchuk, I.V.: Laminar heat and mass transfer in rotating cone-and-plate devices. J. Heat Transfer 133(2)m 024502 (3 pages) (2011) https://asmedigitalcollection.asme.org/heattransfer/article-abstract/133/2/024502/467918/Laminar-Heat-and-Mass-Transfer-in-Rotating-Cone?redirectedFrom=fulltext
45. KARMAN Th.: Uber laminare und turbulente reibung. Z. angew. Math. Mech. 1, 233–252 (1921) https://doi.org/10.1002/zamm.19210010401
46. Batchelor, G.K.: Note on a class of solutions of the navier-stokes equations representing steady rotationally-symmetric flow. The quarterly journal of mechanics and applied mathematics 4(1), 29–41 (1951) https://doi.org/10.1093/qjmam/4.1.29
47. Stewartson, K.: On the flow between two rotating coaxial disks. In: Mathematical Proceedings of the Cambridge Philosophical Society, vol. 49, pp. 333–341 (1953). https://doi.org/10.1017/S0305004100028437 . Cambridge University Press
48. Pearson, C.E.: Numerical solutions for the time-dependent viscous flow between two rotating coaxial disks. Journal of Fluid Mechanics 21(4), 623–633 (1965) https://doi.org/10.1017/S002211206500037X
49. Helcig, C., Wiesche, S., Shevchuk, I.V.: Prandtl number effect on the laminar convective heat transfer from a rotating disk. Journal of Heat Transfer 139(10), 101702 (2017) https://doi.org/10.1115/1.4036729
50. Mahanthesh, B., Gireesha, B., Prasannakumara, B., Kumar, P.S.: Magneto-thermo-marangoni convective flow of cu-h2o nano-liquid past an infinite disk with particle shape and exponential space based heat source effects. Results in physics 7, 2990–2996 (2017) https://doi.org/10.1016/j.rinp.2017.08.016
51. Basavarajappa, M., Bhatta, D.: Lie group analysis of flow and heat transfer of a nanofluid in cone–disk systems with hall current and radiative heat flux. Mathematical Methods in the Applied Sciences 46(14), 15838–15867 (2023) https://doi.org/10.1002/mma.9429
52. Basavarajappa, M., Bhatta, D.: Study of flow of buongiorno nanofluid in a conical gap between a cone and a disk. Physics of Fluids 34(11) (2022) https://doi.org/10.1063/5.0121642
53. Turkyilmazoglu, M.: Flow and heat simultaneously induced by two stretchable rotating disks. Physics of Fluids 28(4) (2016) https://doi.org/10.1063/1.4945651
54. Turkyilmazoglu, M.: Fluid flow and heat transfer over a rotating and vertically moving disk. Physics of Fluids 30(6) (2018) https://doi.org/10.1063/1.5037460
55. Moatimid, G.M., Mohamed, M.A., Elagamy, K.: A casson nanofluid flow within the conical gap between rotating surfaces of a cone and a horizontal disc. Scientific Reports 12(1), 11275 (2022) https://doi.org/10.1038/s41598-022-15094-w
56. Srilatha, P., Remidi, S., Nagapavani, M., Singh, H., Prasannakumara, B.: Heat and mass transfer analysis of a fluid flow across the conical gap of a cone-disk apparatus under the thermophoretic particles motion. Energies 16(2), 952 (2023) https://doi.org/10.3390/en16020952
57. Gul, T., Kashifullah, Bilal, M., Alghamdi, W., Asjad, M.I., Abdeljawad, T.: Hybrid nanofluid flow within the conical gap between the cone and the surface of a rotating disk. Scientific Reports 11(1), 1180 (2021) https://doi.org/10.1038/s41598-020-80750-y
58. Zafar, M., Sakidin, H., Sheremet, M., Dzulkarnain, I.B., Hussain, A., Nazar, R., Khan, J.A., Irfan, M., Said, Z., Afzal, F., *et al.*: Recent development and future prospective of tiwari and das mathematical model in nanofluid flow for different geometries: A review. Processes 11(3), 834 (2023) https://doi.org/10.3390/pr11030834
59. Shevchuk, I.V.: Convective heat and mass transfer in rotating disk systems 45 (2009) https://doi.org/10.1007/978-3-642-00718-7
60. Turkyilmazoglu, M.: On the fluid flow and heat transfer between a cone and a disk both stationary or rotating. Mathematics and Computers in Simulation 177, 329–340 (2020) https://doi.org/10.1016/j.matcom.2020.04.004
61. Srinivas, S., Vijayalakshmi, A., Reddy, A.S.: Flow and heat transfer of gold-blood nanofluid in a porous channel with moving/stationary walls. Journal of Mechanics 33(3), 395–404 (2017) https://doi.org/10.1017/jmech.2016.102
62. Hussain, A., Sarwar, L., Rehman, A., Akbar, S., Gamaoun, F., Coban, H.H., Almaliki, A.H., Alqurashi, M.S.: Heat transfer analysis and effects of (silver and gold) nanoparticles on blood flow inside arterial stenosis. Applied Sciences 12(3), 1601 (2022) https://doi.org/10.3390/app12031601
63. Oberlack, M.: Asymptotic expansion, symmetry groups, and invariant solutions of laminar and turbulent wall-bounded flows. ZAMM-Journal of Applied Mathematics and Mechanics/Zeitschrift für Angewandte Mathematik und Mechanik: Applied Mathematics and Mechanics 80(11-12), 791–800 (2000) https://doi.org/10.1002/1521-4001(200011)80:11/12<791::AID-ZAMM791>3.0.CO;2-5
64. Shampine, L.F., Gladwell, I., Thompson, S.: Solving odes with matlab (2003)

Publisher's Note Springer Nature remains neutral with regard to jurisdictional claims in published maps and institutional affiliations.

Springer Nature or its licensor (e.g. a society or other partner) holds exclusive rights to this article under a publishing agreement with the author(s) or other rightsholder(s); author self-archiving of the accepted manuscript version of this article is solely governed by the terms of such publishing agreement and applicable law.